Generalized paradox of enrichment: noise-driven rare rarity in degraded ecological systems

Shirin Panahi[a], Ulrike Feudel[b], Karen C. Abbott[c], Alan Hastings[d], and Ying-Cheng Lai[a,e,1]

[a]School of Electrical, Computer and Energy Engineering, Arizona State University, Tempe, Arizona 85287, USA; [b]Institute for Chemistry and Biology of the Marine Environment, Carl von Ossietzky University Oldenburg, Carl von Ossietzky-Str. 9-11, Oldenburg 26111, Germany; [c]Department of Biology, Case Western Reserve University, 10900 Euclid Avenue, Cleveland, OH 44106, USA; [d]Department of Environmental Science and Policy, University of California, One Shields Avenue, Davis, CA 95616, USA and Santa Fe Institute, 1399 Hyde Park Road, Santa Fe, NM 87501, USA; [e]Department of Physics, Arizona State University, Tempe, Arizona 85287, USA

This manuscript was compiled on December 12, 2024

The paradox of enrichment is referred to as the counterintuitive phenomenon in ecology where increasing the resources available to the prey population can lead to instability and a higher likelihood of population fluctuations. We study the converse situation where the prey's environment is degrading as caused by, e.g., climate change, and ask if the dynamical interplay between this degradation and stochasticity might actually be beneficial to stabilization of the prey population. The underlying dynamical systems are nonautonomous and subject to noise, and we uncover a phenomenon pertinent to the paradox of enrichment: rare rarity. In particular, in a slow-fast ecosystem with a sole stable equilibrium, noise can induce dynamical excursions of a trajectory into a region with low or near-zero species abundance, resulting in rarity. Surprisingly, it is the same noise that can facilitate a rapid recovery of the abundance of the rare species, making short the duration of the rarity in comparison with the time interval between two adjacent rare-rarity events. As the environment continues to degrade, the occurrence of such rarity events can be nonuniform in time and even more rare. The intermittent occurrence of rare rarity is caused by the dynamical interplay between the phase-space distance from the stable equilibrium to the boundary separating two distinct regions of transient dynamics: one resulting in trajectories directly to the stable equilibrium and another to trajectories a region of near-zero prey abundance. The rare-rarity phenomenon can also arise in other natural systems such as the climate carbon-cycle system.

Paradox of enrichment | Species Rarity | Nonautonomous dynamical system

Consumer-resource interactions often exhibit cycles of prey over exploitation, crash, and recovery. When the prey population's growth capacity is sufficiently low due, for example, to limited resources or poor habitat quality, these cycles are expected to dampen out over time and the system will approach a stable equilibrium point. Enrichment of the prey's environment destabilizes this equilibrium via a Hopf bifurcation. The more favorable conditions allow for a larger and faster prey recovery after over exploitation, resulting in large, sustained oscillations. This is known in ecology as the paradox of enrichment: the counterintuitive phenomenon where increasing the availability of resources, such as nutrients in an ecosystem, can lead to instability and a higher likelihood of population fluctuations in consumer-resource systems (1–7). In this paper, we consider the converse situation where the prey's environment is degrading and ask if the interplay between the direct negative impacts of this degradation and stochasticity might actually lead to stabilization of the prey population. In particular, we shall demonstrate that the nonlinear dynamical effect of the degradation can lead to species rarity but noise can play the beneficial role of quick recovery, a phenomenon that we call "rare rarity."

Species rarity is characterized by a low abundance of certain species, which can be induced by multiple mechanisms. For example, global climate change is having significant impacts on ecological systems on different scales, resulting in slow and gradual deterioration of the species population and eventually leading to rarity. A tipping-point transition (e.g., a saddle-node bifurcation) is a dynamical mechanism that can lead to rarity: the species abundance decreases suddenly to a near-zero level as a parameter of the system passes through a critical point. In a neighborhood beyond a Hopf bifurcation leading to stable oscillations of the population density, at least one population size becomes small in size for a certain time interval corresponding to transient rarity during the limit cycle. In fast-slow and excitable systems, another mechanism of rarity can arise: it can be induced by a trajectory visiting a phase-space region with low species abundance - the phenomenon of dynamical excursion. (Some background topics pertinent to this work are presented in SI Appendix (Sec. I), which include recovery from rarity, tipping, dynamical excursion, noise in ecological systems.)

We focus on species rarity caused by dynamical excursions and find that demographic noise, multiplicative noise that arises commonly in ecological systems, can make the rarity "rare" in time by facilitating a rapid recovery of the abundance after the excursion, thereby preventing extinction. More specifically, we present a rarity phenomenon in a noisy slow-fast

Significance Statement

The counterintuitive phenomenon in ecology that increasing the resources available to the prey population can lead to instability and a higher likelihood of population fluctuations is known as the paradox of enrichment. In the converse situation where the prey's environment is degrading as caused by, e.g., climate change, such a paradox but in a generalized sense can arise: the dynamical interplay between this degradation and stochasticity might actually be beneficial to stabilization of the prey population. It is the collective actions of transients, non-autonomous dynamics, and ecological noise that lead to this surprising phenomenon of rare rarity, with implications to understanding and managing complex ecosystems. The phenomenon can also arise in other natural systems such as the climate carbon cycles.

All conceived the idea. SP performed computations. All analyzed data. YCL and SP wrote the paper. YCL, UF and SP edited the paper.

[1]To whom correspondence should be addressed. E-mail: Ying-Cheng.Lai@asu.edu

predator-prey system. The system is subject to continuous parameter change with time caused by, e.g., environmental changes, and stochastic disturbances modeled by ecologically realistic demographic noise. In the absence of noise, the parameter changes can cause the system to evolve towards a dynamical excursion, after which the species abundances become near zero, making them rare. Demographic noise can facilitate a quick recovery process of the rare species to a high abundance level. As a result, an intermittent behavior can emerge: the system undergoes an excursion again, generating rarity, followed by a fast recovery, and so on. A surprising finding is that, due to the demographic noise, the time duration in which the system exhibits species rarity is relatively short compared to the time interval between two adjacent rare-rarity events, i.e., the excursion-induced rarity is rare! The species are resilient in the sense that, in a long time interval, on average they are able to maintain a high abundance level, in spite of occasionally or intermittently becoming rare. The phenomenon of rare rarity is also found in a stochastic carbon-cycle system [SI Appendix (Sec. II)], suggesting the generality of this phenomenon in nonlinear slow-fast ecological and physical systems.

Results

Slow-fast predator-prey model. We consider a variant of the slow-fast Rosenzweig-MacArthur predator-prey system (8), subject to demographic noise and parameter variations with time (e.g., as the result of environmental change). For simplicity, we assume that the resources available to the prey species in its habitat decline continuously and linearly with time. The nonautonomous dynamical system subject to multiplicative noise is described by the following set of stochastic differential equations:

$$\kappa\dot{x} = x(1-\phi x) - \frac{xy}{1+\eta x} + \xi\sqrt{x}dB(t) \quad [1a]$$

$$\dot{y} = \frac{xy}{1+\eta x} - y + \xi\sqrt{y}dB(t) \quad [1b]$$

$$\dot{\phi} = \begin{cases} r, & \phi_{\min} < \phi < \phi_{\max} \\ 0, & \text{otherwise,} \end{cases} \quad [1c]$$

where x and y are the populations of the fast (prey) and slow (predator) species, respectively, $0 < \kappa \ll 1$ quantifies the time-scale separation between the prey's and predator's life span, η is the predator's interaction time with the prey, and the term $\xi\sqrt{y}dB(t)$ describes the demographic noise with ξ as the noise amplitude and $dB(t)$ being an independent Gaussian random process of zero mean and unit variance (9, 10). Let ϕ be the time-dependent bifurcation parameter that is inversely proportional to the carrying capacity of the prey habitat. It varies linearly with time at the rate r from $\phi_{\min}$ initially to $\phi_{\max}$ after certain time. As $\phi(t)$ increases with time, the carrying capacity of the prey habitat deteriorates continuously, so $\phi(t)$'s increase with time could, roughly, be the result of the ever increasing human influences on the ecosystem. The three quantities, r, $\phi_{\min}$ and $\phi_{\max}$ define a proper or calibrating time scale of the nonautonomous dynamical system Eq. (1):

$$T_s \equiv \frac{\phi_{\max} - \phi_{\min}}{r}, \quad [2]$$

with which the duration of various dynamical events of the system can be compared. The quantity T_s is the time interval over which an environmental change is assumed to happen. We integrate the nonautonomous system Eq. (1) using a standard second-order method for stochastic differential equations (11).

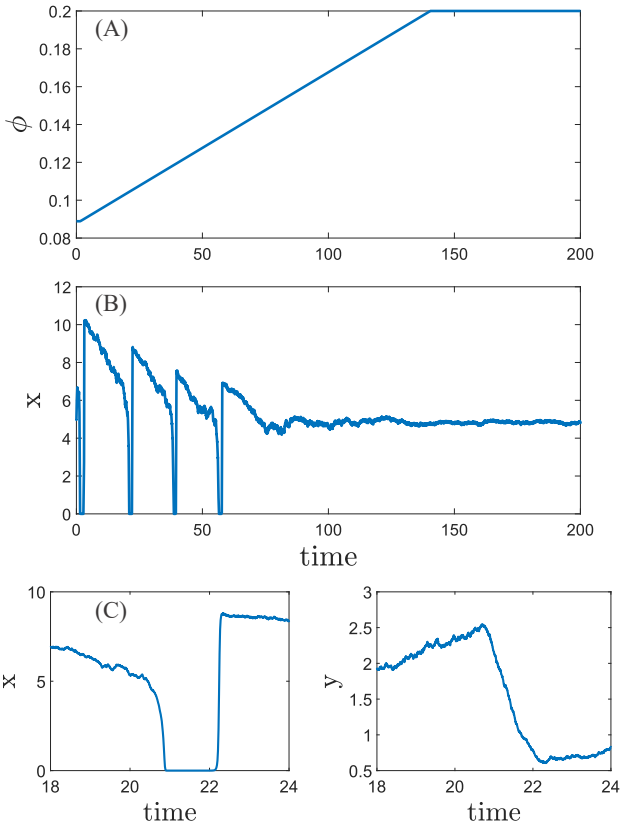

Fig. 1. Demonstration of the phenomenon of the rare rarity of the prey population in the nonautonomous predator-prey system Eq. (1). (a) Time-varying parameter $\phi(t)$, which is inversely proportional to the carrying capacity and increases linearly from $\phi_{\min} \approx 0.09$ at $t = 0$ to $\phi_{\max} \approx 0.2$ at the rate $r = 0.0002$. (b) A representative time series (a random realization) of the prey population for $\eta = 0.8$ and $\kappa = 0.01$. The amplitude of the demographic noise is $\xi = 0.1$. For this realization, during the time interval in which the capacity parameter ϕ changes, there are four occurrences of the rarity of the prey population. (c) A magnification of a typical rarity event, which lasts for a quite short time relative to the system time scale T_s, signifying "rare rarity." (d) The corresponding Time series $y(t)$ of the predator population.

Rare rarity in the prey population. Figure 1(A) shows the time-varying parameter $\phi(t)$ for $r = 0.0002$, $\phi_{\min} = 0.09$, and $\phi_{\max} = 0.199$. The corresponding time series of the prey population $x(t)$ is shown in Fig. 1(B) for $\eta = 0.8$ and $\kappa = 0.01$, and noise amplitude $\xi = 0.1$. During the time interval in which the control parameter ϕ varies, there are four occurrences of rarity in which the prey population reaches a dangerously low, near-zero level. The remarkable feature is that each occurrence of rarity lasts only for a relatively short time, as exemplified in Fig. 1(C), a magnification of one of the rarity events. The rarity event lasts for a short time in the sense that, in terms of the calibrating time T_s, the duration of the rarity event is less than 1%. Figure 1(C) also shows that, after temporally approaching some near zero value, the prey population quickly recovers to the normal level. Such a rarity event can thus be regarded as a "quick" transient event of temporary population collapse. In the entire observational

time interval, the total duration of all rarity events is thus short, rendering *rare* the rarity events. In fact, the length of the rarity interval is related to the intrinsic time scales of the predator-prey system determined by the parameter κ that characterizes the time-scale separation between the lifetimes of the two species: predator and prey. In general, the life spans on different trophic levels follow an allometric slowing down (12), i.e., species on a higher trophic level (here the predator) grow slower than the species on lower trophic levels (the prey). Note that, in spite of the rare rarity occurrences of the prey population, the predator population maintains at a level well away from zero, as shown in Fig. 1(D).

The time series exemplified in Fig. 1(B) is one random realization of the underlying stochastic dynamical system. To statistically characterize the phenomenon of rare rarity, we define two quantities: (1) ΔT_c, the time interval between two adjacent rare-rarity events, and (2) N_c, the number of occurrences of such events in the time interval $[0, T_s]$. The statistics of the two quantities can be obtained from a large number of dynamical realizations. Figures 2(A) and 2(B) show a histogram of ΔT_c on a linear and logarithmic scale, respectively, from 800 independent realizations. It can be seen that the distribution of ΔT_c is algebraic or power-law, which is characteristic of typical intermittent behavior in nonlinear dynamical systems (13). The corresponding histogram of N_c is shown in Fig. 2(C), which is approximately Gaussian with the mean value $\langle N_c \rangle \approx 8$ and variance $\sigma_{N_c} \approx 3$. As the rate r of parameter change increases, on average the number of occurrences of rare rarity decreases, due to the reduction in the time duration T_s of the parameter variation, as shown in Fig. 2(D).

Dynamical mechanism of rare rarity: a deterministic autonomous approach. To uncover the dynamical mechanism for the phenomenon of rare rarity as exemplified in Figs. 1 and 2, it is necessary to examine the global phase-space structure (8) and study the corresponding autonomous deterministic system of Eq. (1) with the bifurcation parameter ϕ:

$$\kappa \dot{x} = x(1 - \phi x) - \frac{xy}{1 + \eta x} \qquad [3a]$$

$$\dot{y} = \frac{xy}{1 + \eta x} - y, \qquad [3b]$$

which is a slow-fast system. We choose the value of ϕ from an interval in which both the average prey and predator populations are nonzero. For a perfect time-scale separation of predator and prey, $\kappa = 0$, we can compute the stability of the critical manifold by transforming the system Eq. (3) in slow time t into fast time $\tau = \kappa t$, leading to

$$\dot{x} = x(1 - \phi x) - \frac{xy}{1 + \eta x} \qquad [4a]$$

$$\dot{y} = \kappa \left(\frac{xy}{1 + \eta x} - y \right), \qquad [4b]$$

where the dot now indicates the derivative with respect to τ. The independent variables t and τ correspond to the fast and slow times, respectively, with Eq. (3) and Eq. (4) being the fast and slow systems, respectively, which are equivalent for $\kappa \neq 0$.

In the limit $\kappa = 0$, the predator population y is constant, and only the fast dynamics of the prey x need to be considered, which can be approximated by a one-dimensional critical

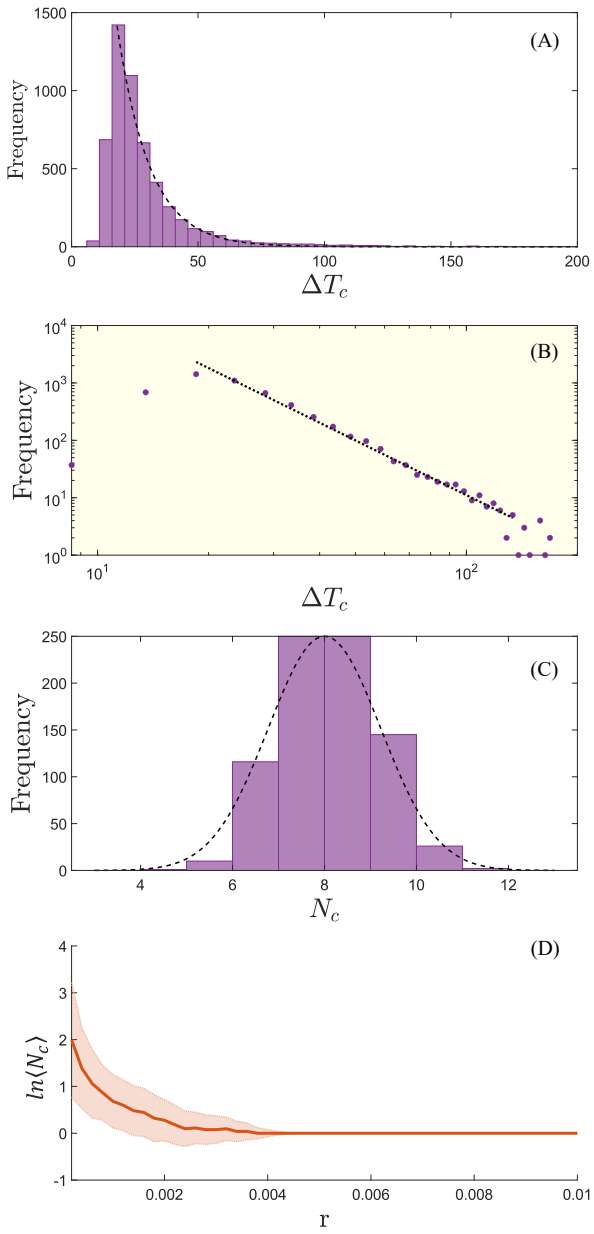

Fig. 2. Statistical characterization of rare rarity. (A, B) Distribution of ΔT_c, the time interval between two adjacent rare-rarity events, on a linear and logarithmic scale, respectively, for $r = 0.0002$. (C) Distribution of N_c, the number of rare-rarity events during the time interval of parameter variation for $r = 0.0002$. (D) The mean value $\langle N_c \rangle$ versus the rate of parameter change. Other parameters are the same as in Fig. 1. For clarity, $\langle N_c \rangle$ is plotted on a logarithmic scale, while the shaded area represents the standard deviation on a linear scale.

manifold (or the x-nullcline of the system) (14–16):

$$M_s = \{(x, y) \in R^2 | x = 0, y = (1 - \phi x)(1 + \eta x)\}, \qquad [5]$$

where the first component is a line perpendicular to the fast direction and the second (fold) component is a curve with a fold tangent to the fast direction at the point

$$(x_f, y_f) = ((\eta - \phi)/2\eta\phi, (\eta + \phi)^2/4\eta\phi).$$

To elaborate, the critical manifold M_s consists of the steady states of Eq. (4) with $\kappa = 0$, whose stability can be determined.

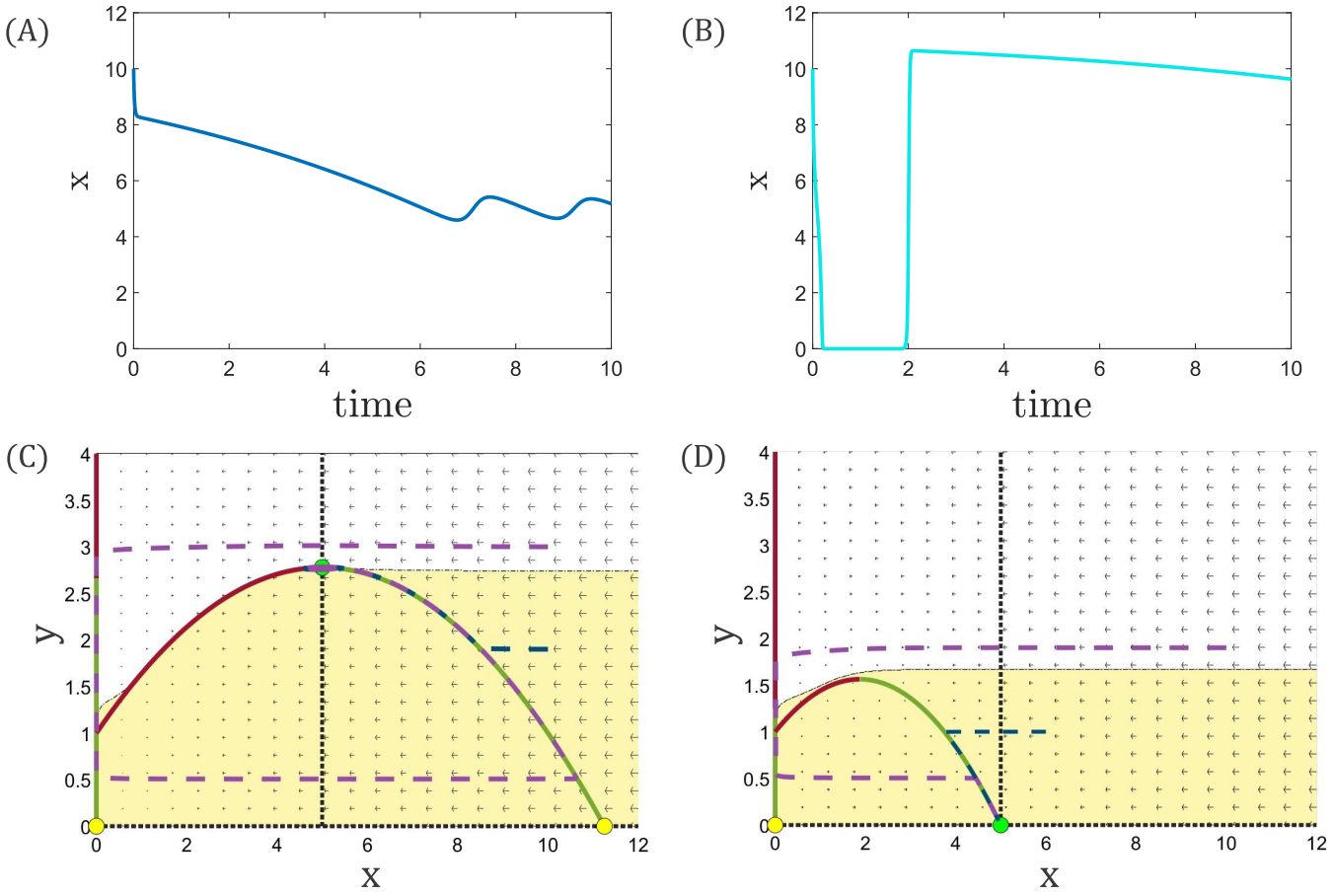

Fig. 3. Phase-space structure of the deterministic predator-prey model Eq. (3). Two representative time series of the prey population from two different initial conditions: (A) $[10, 2]$ and (B) $[10, 3]$ for $\eta = 0.8$, $\phi = 0.09$, $\kappa = 0.01$, and $\xi = 0.1$. For (A), the prey population is maintained at a healthy level in the time window of observation. For (B), rarity arises because the prey population becomes near zero for a short transient period of time. (C) Phase-space structure for $\phi = 0.09$, where the white region corresponds to the excursive initial points that undergo temporary collapse of the prey population, leading to rarity, and the initial conditions in the yellow region lead to trajectories that go directly into the sole global stable equilibrium (the filled green circle) without the occurrence of rarity. Since the stable equilibrium is on the boundary between the white and yellow regions, noise with an arbitrary amplitude can land the system into the white region, generating rarity, after which the system settles into stable equilibrium again. This process can repeat, generating the intermittent rarity behavior as exemplified in Fig. 1(B) in the time period in which the control parameter ϕ varies with time but its values are relatively small. (D) Phase-space structure for $\phi = 0.199$. In this case, the stable equilibrium is near the x-axis and is far away from the boundary between the white and yellow regions. While the white region becomes larger as compared with that in (C), noise with an extraordinarily large amplitude is required to kick the system into the white region, making the time to observe such an event prohibitively long, as demonstrated in Fig. 1(B).

The fold component has a stable and an unstable part with a saddle-node bifurcation at the fold point. The other part of the critical manifold, the y axis as a vertical line, is stable but it becomes unstable below the intersection point with the other part of M_s. This view provides a picture of the direction of the trajectories in that limit, which is only slightly different for $0 < \kappa << 1$.

The equilibria of the system Eq. (4) are located at the intersections of the x- and y-nullclines. Consider the parameter setting in which the system Eq. (3) has one globally stable equilibrium in which the predator and prey coexist. Depending on the initial condition, the slow-fast system exhibits distinct transient behaviors. For example, Figs. 3(A) and 3(B) show two time series of the fast variable from two different initial conditions for $\eta = 0.8$, $\phi = 0.09$, $\kappa = 0.01$, and $\xi = 0.1$. The time series in Fig. 3(A) corresponds to some "healthy" behavior of the prey population in the sense that, in spite of the oscillations, a finite population is maintained. However, for a different initial condition, there is a time interval in which the fast variable approaches zero, as shown in Fig. 3(B). The corresponding behavior of rarity lasts for a relatively short period of time before the population recovers to a healthy level. Figure 3(C) shows the phase-space structure of the system Eq. (3) for fixed $\phi = 0.09$ and $\eta = 0.8$, with one globally stable equilibrium (closed green circle) and two unstable equilibria (the two yellow circles). The positions and stability of the equilibria depend on the values of the parameters ϕ and η. The chosen $\phi = 0.09$ is quite close to a Hopf bifurcation at $\phi = 0.088$, which explains the oscillations for the initial condition visible in Fig. 3(A). The dashed vertical black line represents the y-nullcline. The x-nullcline or the critical manifold of the system is shown by a solid line and curve segments, with the stable (unstable) parts in green (red). The intersection points of the y-nullcline and the critical manifold (x-nullcline) give the equilibria of the system.

Depending on the initial condition, there are two distinct

transient behaviors in their convergence to the global stable equilibrium: direct (yellow region) and excursive (white region). For an initial condition from the yellow region, the system approaches the stable equilibrium directly. However, for initial conditions from the excursive region, the system experiences a large excursion in the phase space that includes a close approach to zero populations, leading to a sudden transient collapse in both the predator and prey populations before eventually reaching the stable steady state. Two examples of the dynamical trajectories, one initiated from the white (purple dashed line) and another from the yellow region (blue dashed line), are shown in Fig. 3(C). It can be seen that the dynamical trajectory from the initial condition in the white region approaches the y-axis (zero prey population) and stays near it for a transient period of time before leaving it and approaching the stable equilibrium.

To gain more insights into the state of rarity, we recall that the trajectory approaches the y axis fast where x is near zero. In this case, the dynamic is determined only by the dynamics of the slow variable y. A reasonable approximation for the time scale, which is essential for the motion in the neighborhood of the y axis, can be derived by examining the corresponding trajectories. In particular, setting $x = 0$ in Eq. (3), we obtain $\dot{y} = -y$, whose time scale is short compared to that of the environmental change. The analysis of the dynamics in fast time τ reveals that the intersection between the unstable fold part and the y axis part of M_s is the point at which the downward moving trajectory changes from the influence of the stable to the impact of the unstable part of the critical manifold. This leads to a strong repulsion ending the rarity interval and pushing the system back to large population densities. How strong the attraction to and the repulsion from the y axis depends strongly on the time-scale separation κ.

By including noise in Eq. (4), the initial conditions in the neighborhood of the horizontal line separating the trajectories (basin boundary) possessing initially a rarity event or not can change their behavior due to the noise. The second impact of the noise concerns the time when the intersection point between the two parts of M_s is reached. Due to the closeness to the line of $x = 0$, the noise acts mainly on y shifting the point at which the rarity event is ending. This shift could occur in either direction (either extending or reducing the duration of prey rarity), but because the noise has a proportionally larger impact on small populations, noise-driven reductions in y predominate and so the trend is toward shortening the rarity event.

Figure 1(B) reveals that for a relatively large value of the bifurcation parameter ϕ, the phenomenon of intermittent rare rarity no longer occurs. This can also be understood by examining the phase-space structure of the deterministic system. Figure 3(D) shows, for $\phi = 0.199$, that the system has a stable equilibrium with a near-zero predator population and an unstable equilibrium corresponding to the extinction of both species. In this case, the folded component of the critical manifold shrinks as compared with the case of a smaller value of ϕ, leading to a larger white area. However, differing from the case of a smaller ϕ value in Fig. 3(C), the global stable equilibrium is now far away from the boundary between the white and yellow regions. Once the system settles into the stable equilibrium, a noise realization of extraordinarily large amplitude is required to kick the system into the white region to exhibit the rarity of the prey population. While abnormally large amplitude realizations are possible for demographic noise, it would require a long time to actually experience such a realization. This explains why no rarity events occur for large values of ϕ in Fig. 1(B) in the time window of observation. It is worth noting that, for $\phi = 0.199$, the predator population is near zero all the time, as can be seen from Fig. 3(D) which is due to the fact that this point is close to the transcritical bifurcation point ($\phi = 0.2$) where the predator dies out.

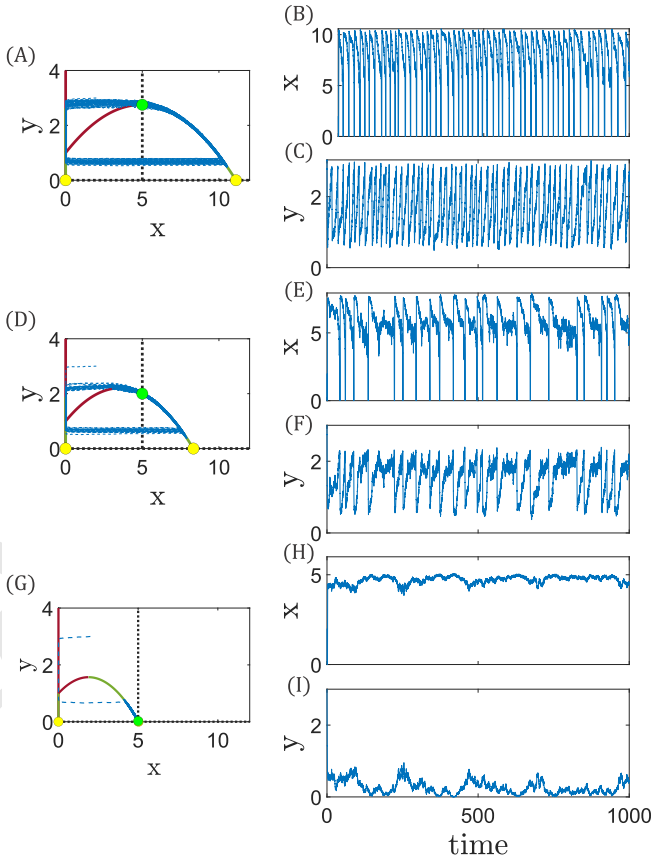

Fig. 4. Role of noise in rare rarity. (A-C) Phase-space trajectories and the corresponding time series of the prey population for $\phi = 0.09$, respectively. The sole stable equilibrium of the system lies close to the boundary between the phase-space regions with distinct transient behavior, so even noise of small amplitude can induce a rare rarity event. (D-F) Same legends as in (A-C) but for $\phi = 0.12$. The stable equilibrium is away from the boundary, requiring larger noise to induce a rare rarity event. This reduces the number of such events in the same time interval as compared with (A-C). (G-I) Same legends as in (A-C) but for $\phi = 0.199$. In this case, the stable equilibrium is far away from the boundary, requiring significantly stronger noise to induce a rare rarity event. No such event occurs in the same time window of observation. Other parameter values are $\eta = 0.8$, $\kappa = 0.01$, and $\xi = 0.1$.

The phase-space structure exemplified in Figs. 3(C) and 3(D) suggests that the distance between the global stable equilibrium and the boundary of the regions with distinct transient dynamical behaviors is key to the occurrence of the rare-rarity events in terms of their frequency and regularity. To verify this explicitly, we compare the trajectories and the corresponding time series of the prey population of the autonomous noisy system for three fixed values of ϕ: $\phi = 0.09$, 0.12, and 0.199, in a long time window, as shown in Fig. 4. For $\phi = 0.09$, the stable equilibrium is approximately on the boundary. In this case, even small noise can drive the system out of the

equilibrium, leading to a transient excursion in the phase space that stays near the y axis (near zero prey population) for some time, as shown in Figs. 4(A). As a result, the rare-rarity events associated with the prey population occur quite frequently, as shown in Fig. 4(B), which leads to oscillation in the predator population as depicted in Fig. 4(C). For $\phi = 0.12$, the position of the stable equilibrium is lower in the phase space as compared with the case of $\phi = 0.09$ and is away from the boundary, as shown in Fig. 4(D), so some larger noise is required to induce a rare-rarity event, making these events more infrequent than the case of $\phi = 0.09$, as shown in Fig. 4(E). The predator population and the number of oscillations also decrease as shown in Fig. 4(F). For $\phi = 0.199$, the stable equilibrium is far away from the boundary, so the dynamical trajectory, once approaching the equilibrium, tends to stay there as the required noise level to kick it out is enormous, as shown in Fig. 4(G). In the time window of observation, there is in fact no rare-rarity event, as shown in Fig. 4(H) and the predator population remains near zero without any oscillation, as can be seen from Fig. 4(I).

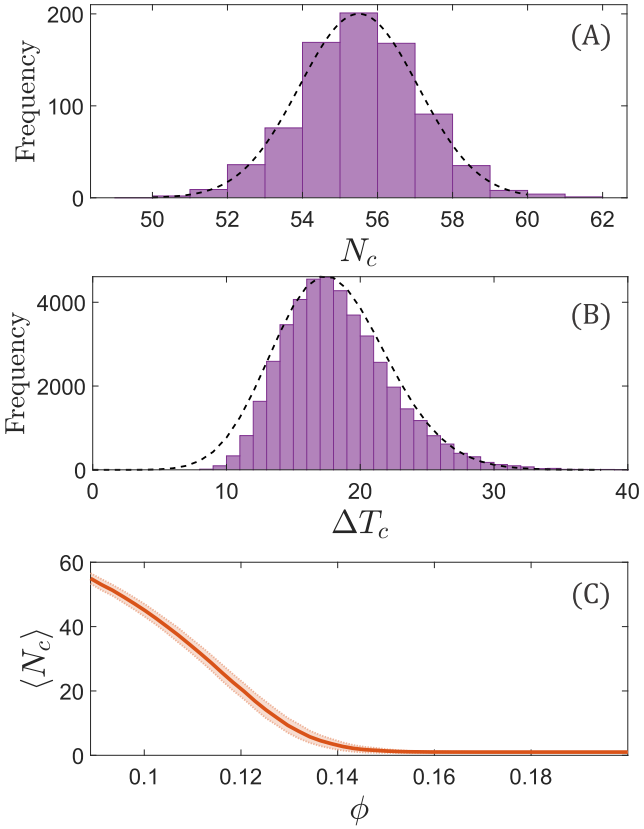

Fig. 5. Statistical behavior of rare rarity events in the autonomous system Eq. (3) subject to demographic noise. (A) Distribution of N_c, the number of rare rarity events in a long observational time window, which is approximately Gaussian. (B) Distribution of ΔT_c, the time interval between two adjacent rare-rarity events, which is approximately Poisson. The system parameter values are $\phi = 0.09$, $\eta = 0.8$, $\kappa = 0.01$, and $\xi = 0.1$. (C) Average value $\langle N_c \rangle$ of rare rarity events versus ϕ. The shaded area indicates the standard deviation of the average.

Figure 5(A) shows the distribution of the number N_c of the rare rarity events in the time interval $[0, 1000]$ in the autonomous noisy model for $\phi = 0.09$, $\eta = 0.8$, $\kappa = 0.01$, and $\xi = 0.1$, which can be approximated by a normal distribution [similar to that from the nonautonomous system Eq. (1) shown in Fig. 2(C)]. Figure 5(B) shows the distribution of ΔT_c, the time interval between two adjacent rare-rarity events, which can be approximated by a Poisson distribution. The most likely time interval between two adjacent rare-rarity events lies in $\Delta T_c \in [16\ 18]$. Figure 5(C) shows the mean value of the approximately Gaussian random variable N_c versus the bifurcation parameter ϕ where, for each fixed value of ϕ, 800 noisy realizations are used to calculate $\langle N_c \rangle$. The decreasing behavior of $\langle N_c \rangle$ with ϕ is similar to that obtained from the nonautonomous system Eq. (1), indicating that species living under poorer environmental conditions (large value of parameter ϕ) tend to retain their abundance and are robust.

Dynamical mechanism of rare rarity: a deterministic nonautonomous approach. The final step is to consider the full nonautonomous system with noise Eq. (1). Due to the time-dependent change of the environmental conditions with the rate r, all stationary states are transformed into quasistationary equilibria that move in the phase space. For equilibrium state in which predator and prey coexist, we have

$$(x_s,\, y_s) = (1/1 - \eta,\, (1 - \eta - \phi(t)/(1 - \eta)^2).$$

Besides the quasistationary state, the critical manifolds M_s as well as the fold $(x_f,\, y_f)$ change their location in the phase space following the environmental change. For this reason, the situation is more complicated since now not all initial conditions converging to the stable critical manifold without a rarity event will track the quasistationary equilibrium, i.e., stay in its neighborhood during the environmental change. As shown previously (8), there are also tipping trajectories that cross the fold and exhibit the collapse-like behavior (excursion), the rarity event. In the phase space, there exists a boundary – a canard trajectory – which separates tracking and tipping trajectories. Now we can have different situations when the noise is acting on those two types of trajectories. A noiseless tipping trajectory can be pushed by the noise over the canard trajectory to make it a trapping trajectory and vice versa. But a tracking trajectory can also be pushed over the fold by the noise. The fourth case could be that the noise prevents tipping. All of those scenarios are possible. We illustrate one of the scenarios by plotting the trajectory shown in Fig. 4 in the full three-dimensional phase space spanned by x, y, and ϕ.

Figure 6 shows two trajectories similar to that one in Fig. 1(B) in 3D including the critical manifold and the canard. The shaded red region represents the stable part of the critical manifold, while the blue area indicates the unstable part. The moving fold point (x_s, y_s) is depicted by a solid black line, and the stable equilibrium is shown with a dashed yellow line. The singular canard is represented by a blue trajectory, and the folded saddle singularity is marked by a yellow circle. Due to the time-scale separation, the noise is acting mainly on the critical manifold, not perpendicular to it. The initial conditions for the green trajectory shown in Fig. 6(A) [magnified in Fig. 6(B)] are selected from the upper region of the critical manifold above the critical canard, where the trajectory exhibits a tipping behavior in a noiseless environment. In contrast, the initial conditions for the trajectory in Fig. 6(C) [magnified in Fig. 6(D)] are chosen from the lower region of the critical manifold, in which in a noiseless environment resulting in a trapping behavior. As a result, if the initial condition

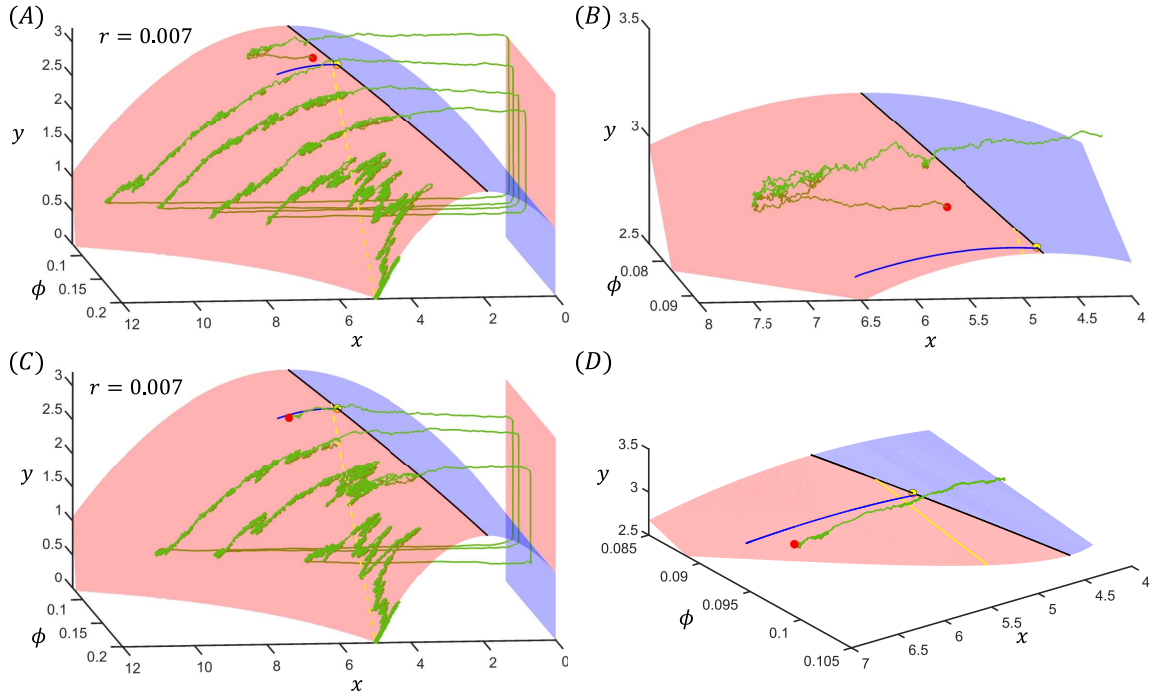

Fig. 6. Critical manifold M_s of the nonautonomous system Eq. (4) and its stability. The shaded red (blue) region represents the stable (unstable) parts, the moving fold point (x_s, y_s), and the stable equilibrium is depicted by a solid black line and a dashed yellow line, respectively. The singular canard is represented by a blue trajectory, and the folded saddle singularity is marked by a yellow circle. Green curves illustrate trajectories corresponding to the initial conditions (A) above and (C) below the singular canard (the initial condition in depicted with a red dot). Panels (B) and (D) provide magnified views of (A) and (C), respectively, for clarity.

is chosen from the lower part, noise will first kick the system over the fold, and then the system returns after the rarity event back to the critical manifold but further down as ϕ has changed. It will get pushed by the noise to more rarity events until it ends up too far from the fold where the noise cannot push the system over the fold, as shown in Fig. 1(B).

Discussion

The key parameters of an ecosystem can depend on time, and this time dependence becomes increasingly more relevant due to the systematic and persistent climate and environmental changes caused mostly by human activities. To model realistic ecosystems as accurately as possible, a description based on nonautonomous dynamical systems (17–24) becomes more meaningful and even necessary. Ecosystems are also subjected to noise, including multiplicative demographic noises. The study of rate-dependent phenomena in conjunction with noise can lead to unexpected phenomena as studies of the interplay between noise-induced and rate-induced tipping show (25). This work reports another phenomenon: rare rarity in ecosystems. In particular, rarity as characterized by some key dynamical variable approaching a near-zero value can arise in slow-fast as well as in excitable dynamical systems when a trajectory visits a phase-space region containing the zero point of this dynamical variable. Such an excursion can be induced by a time-dependent variation of a control parameter as well as by noise. There are two possible mechanisms that can "kick" the system out of this region close to zero: one is the noise and another is the time-scale separation between the different components in a slow-fast system. Both mechanisms can make the dynamical event last for a short time only in comparison with the typical time scale of environmental change. Both noise and time-scale separation coupled with nonautonomy play the role of a double-edged sword: driving the system into rarity and then quickly away from it, making the rarity event rare. As a bifurcation parameter changes with time, the "barrier" for the trajectory to cross to reach the rarity region can become higher, making rarity events even more rare. This explains our counterintuitive result that even when the parameter change is in itself detrimental (e.g., degradation of the prey's carrying capacity), it can protect the population from excursions to rarity. This stabilizing effect is related to the paradox of enrichment, but in reverse.

We have uncovered this phenomenon of rare rarity in two nonautonomous dynamical systems subject to noise: a variant of the slow-fast Rosenzweig-MacArthur predator-prey system and a climate carbon-cycle system, and developed an initial theoretical understanding of the phenomenon through a phase-space analysis of the stochastic dynamical trajectories. A common dynamical feature for rare rarity to arise is the existence of a sole stable equilibrium. Due to excitability or in slow-fast systems with curved critical manifolds, two distinct regions of transient dynamics can arise: one resulting in trajectories going directly to the stable equilibrium and another leading to trajectories that experience an excursion to a different region in the phase space, e.g., a region of near-zero prey abundance in population dynamical systems, before approaching the stable equilibrium. The distance between the stable equilibrium and the boundary separating the two distinct regions is the key to the dynamical interplay between nonautonomy and noise: as a bifurcation parameter changes, the distance can increase/decrease, thereby requiring stronger/weaker noise to

drive the system into the rarity region. When observing the occurrence of the rarity events with time, one typically finds a nonuniform type of intermittent behavior as the frequency by which such events occur decreases continuously with time [e.g., Fig. 1(B)]

The duration of rarity events was studied in Ref. (26) using a similar predator-prey model, except without time-scale differences and under constant parameter values. Without time-scale separation, the predator also becomes rare during epochs of prey rarity. As a result, the trajectory passes much more closely in phase space to the saddle points at joint extinction $(0, 0)$ and predator extinction $(1/\phi, 0)$ [the yellow circles in Figs. 3(C), 4(A), and 4(D)]. Because the dynamics slow near saddles, the closer the stochastic trajectory comes to these saddles, the longer it takes for the populations to recover and complete the cycle. Quick recovery from rarity therefore occurs in part due to the slowness of the predator decline, which keeps trajectories from approaching near enough to the $y = 0$ axis to be trapped in a long transient by the saddle. Future work to explore how much time-scale separation is needed for the behavior to switch from a delayed recovery (as in Ref. (26)) to a rapid recovery (as shown here) from rarity would be informative.

In ecological systems, the relevant source of stochastic influence is often demographic noise and the time scales of the predator and prey variables typically differ drastically. As a result, the phenomenon of rare rarity can occur, where the prey population density decreases quickly to a near-zero value, followed by a rapid recovery. Rare rarity is triggered by the interplay between noise and the intrinsic slow-fast dynamics of the system coupled to time-dependent environmental changes, such that when a species becomes rare, a quick recovery can occur. This suggests that in slow-fast ecological systems, habitat degradation can act as a double-edged sword with both negative and beneficial effects on the prey population. Environmental deterioration due to climate change can cause a decrease in the prey carrying capacity but, surprisingly, it also reduces the probability of rate rarity events in the prey population. A similar phenomenon was found in a prototypical excitable climate-carbon cycle system with additive noise [SI Appendix (Sec. II)], suggesting the generality of the phenomenon.

ACKNOWLEDGMENTS. The work at Arizona State University was supported by AFOSR under Grant No. FA9550-21-1-0438.

1. Michael L Rosenzweig. Paradox of enrichment: destabilization of exploitation ecosystems in ecological time. *Science*, 171(3969):385–387, 1971.
2. S. Roy and J. Chattopadhyayy. The stability of ecosystems: A brief overview of the paradox of enrichment. *J. Biosci.*, 1971:421–428, 1971.
3. Robert May. Limit cycles in predator–prey communities. *Science*, 177:900–902, 1972.
4. Michael Gilpin and Michael Rosenzweig. Enriched predator–prey systems: Theoretical stability. *Science*, 177:902–904, 1972.
5. Marten Scheffer and Rob J. De Boer. Implications of spatial heterogeneity for the paradox of enrichment. *Ecology*, 76(7):2270–2277, October 1995. ISSN 1939-9170. . URL http://dx.doi.org/10.2307/1941701.
6. Shovonlal Roy and J Chattopadhyay. The stability of ecosystems: a brief overview of the paradox of enrichment. *J. Biosci.*, 32:421–428, 2007.
7. Kot. Mark. *Elements of Mathematical Ecology*. Cambridge University Press, New York, 2001.
8. Anna Vanselow, Sebastian Wieczorek, and Ulrike Feudel. When very slow is too fast-collapse of a predator-prey system. *J. Theo. Biol.*, 479:64–72, 2019.
9. Michael B. Bonsall and Alan Hastings. Demographic and environmental stochasticity in predator–prey metapopulation dynamics. *J. Animal Ecol.*, 73(6):1043–1055, 2004.
10. Haim Weissmann, Nadav M. Shnerb, and David A. Kessler. Simulation of spatial systems with demographic noise. *Phys. Rev. E*, 98:022131, Aug 2018. .
11. Christian Van den Broeck, JMR Parrondo, Raúl Toral, and Ryoichi Kawai. Nonequilibrium phase transitions induced by multiplicative noise. *Phys. Rev. E*, 55(4):4084, 1997.
12. Geoffrey B West, James H Brown, and Brian J Enquist. A general model for ontogenetic growth. *Nature*, 413(6856):628–631, 2001.
13. E. Ott. *Chaos in Dynamical Systems*. Cambridge University Press, Cambridge, UK, second edition, 2002.
14. J. Guckenheimer and P. J. Holmes. *Nonlinear Oscillations, Dynamical Systems, and Bifurcations of Vector Fields*. Springer, New York, 1983.
15. Neil Fenichel. Geometric singular perturbation theory for ordinary differential equations. *J. Differ. Equ.*, 31(1):53–98, 1979.
16. Jean-Marc Ginoux. Slow invariant manifolds of slow–fast dynamical systems. *Int. J. Bifurcat. Chaos*, 31(07):2150112, 2021.
17. Sebastian Wieczorek, Peter Ashwin, Catherine M Luke, and Peter M Cox. Excitability in ramped systems: the compost-bomb instability. *Proc. R. Soc. A Math. Phys. Eng. Sci.*, 467 (2129):1243–1269, 2011.
18. P. Ashwin, S. Wieczorek, R. Vitolo, and P. Cox. Tipping points in open systems: bifurcation, noise-induced and rate-dependent examples in the climate system. *Phil. Trans. Roy. Soc. A*, 370:1166–1184, 2012.
19. Peter Ashwin, Clare Perryman, and Sebastian Wieczorek. Parameter shifts for nonautonomous systems in low dimension: bifurcation-and rate-induced tipping. *Nonlinearity*, 30(6):2185, 2017.
20. B. Kaszás, U. Feudel, and T Tél. Tipping phenomena in typical dynamical systems subjected to parameter drift. *Sci. Rep.*, 9:8654, 2019.
21. Dániel Jánosi, G. Károlyi, and Tamás Tél. Climate change in mechanical systems: the snapshot view of parallel dynamical evolutions. *Nonlinear Dyn.*, 106:2781–2805, 2021.
22. Dániel Jánosi and Tamás Tél. Characterizing chaos in systems subjected to parameter drift. *Phys. Rev. E*, 105:L062202, Jun 2022. . URL https://link.aps.org/doi/10.1103/PhysRevE.105.L062202.
23. U. Feudel. Rate-induced tipping in ecosystems and climate: the role of unstable states, basin boundaries and transient dynamics. *Nonlinear Proc. Geophys.*, 30(4):481–502, 2023. . URL https://npg.copernicus.org/articles/30/481/2023/.
24. Anna Vanselow, Lukas Halekotte, Pinaki Pal, Sebastian Wieczorek, and Ulrike Feudel. Rate-induced tipping can trigger plankton blooms. *Theo. Ecol.*, 2024. .
25. Katherine Slyman and Christopher K. Jones. Rate and noise-induced tipping working in concert. *Chaos*, 33(1):013119, 01 2023. ISSN 1054-1500. . URL https://doi.org/10.1063/5.0129341.
26. Jonathan E Rubin, David JD Earn, Priscilla E Greenwood, Todd L Parsons, and Karen C Abbott. Irregular population cycles driven by environmental stochasticity and saddle crawlbys. *Oikos*, 2023(2):e09290, 2023.

PNAS

Supporting Information for

Generalized paradox of enrichment: Noise-driven rare rarity in degraded ecological systems

Shirin Panahi, Ulrike Feudel, Karen C. Abbott, Alan Hastings, and Ying-Cheng Lai[1]

[1]To whom correspondence should be addressed. E-mail: Ying-Cheng.Lai@asu.edu

This PDF file includes:

Supporting Information Text

1. Pertinent background

A. Recovery from rarity. Understanding how rare species avoid extinction is critical for conservation. For species that are chronically rare, persistence has been attributed to factors such as high local abundances (despite very low regional abundance) (1), reproductive adaptations that offset low encounter rates with potential mates (2), and dispersal and niche shifts (3). For species that only experience rarity during acute collapse events, such as those that we considered in this study, extinction avoidance relies on fast recovery. In single-species populations, this can be accomplished by a high intrinsic growth rate (4). In multi-species communities, recovery requires not only that the rare species can grow quickly, but that it can do so under the specific pressures being imposed by interacting species (5). In continually deteriorating environments, rare species must also be able to recover under worse environmental conditions as those that may have caused the collapse to rarity in the first place (6).

B. Tipping in ecological systems. In an ecological system with two coexisting stable equilibria (stable steady states or fixed-point attractors), one associated with healthy survival while the other with extinction, as a parameter changes through a critical point, an inverse saddle-node bifurcation can occur, beyond which the survival attractor no longer exists, leaving the extinction attractor as the only final steady state of the system. This leads to a tipping point at which the species abundances decrease to near-zero values (7–32), which can be considered as below an empirical extinction threshold (33). Besides population dynamics in ecology, tipping points are relevant to phenomena in other fields such as epidemic outbreak (34), climate change (35), and the sudden switch from normal to depressed mood in bipolar patients (36).

When the parameters of a system vary with time, rate-induced tipping (R-tipping) can occur (16, 37–40). In particular, for certain initial conditions leading to trajectories approaching the survival equilibrium attractor in the absence of time-dependent parameters, a population with these initial conditions can become extinct if some parameters change too fast with time. The rate of parameter change thus becomes a key "hyperparameter" of the system: as it increases through a critical value, some initial conditions will switch their destination from healthy survival to extinction. It was recognized that the rate of environmental change is effectively a parameter affecting the dynamics across different scales in ecology (41). In a recent study focusing on complex ecological networks (42), a global approach to R-tipping was introduced with the finding that the probability of R-tipping defined with respect to initial conditions taken from the entire relevant phase-space region can increase rapidly as soon as the rate of parameter changes becomes nonzero. For simple fast-slow systems, one can identify even a boundary in the phase space – a canard trajectory – which separates tipping from tracking (i.e., following the survival state) initial conditions (38, 40, 43). Besides population dynamics, the phenomenon of R-tipping is relevant to fields such as climate science (44, 45), neuroscience (43, 46), vibration engineering (47), and even competitive economy (48).

C. Dynamical excursion in slow-fast and excitable systems. In ecological systems, another mechanism for rarity can arise in slow-fast (38) and excitable systems (40, 43, 49, 50). In an early work (49) on a predator-prey model with a Holling type-III predator response, it was found that noise can sustain a transient in the setting that the system has only one globally stable equilibrium. There are two distinct types of trajectories: one that reaches the equilibrium directly and another approaching the equilibrium through an excursive behavior with a sudden but transient excursion away from the equilibrium in both the predator and prey populations. During the excursion, the prey population can reach a near-zero level, resulting in rarity. When noise is present, an intermittent behavior can arise between low-amplitude random oscillations around the equilibrium and the infrequent high-amplitude oscillations away from the equilibrium. In a more recent work (38) on the Rosenzweig-MacArthur predator-prey model, the impact of a specific type of time-dependent parameter change (a linear reduction of the habitat quality over time) on the transient response of the slow-fast dynamics was studied. It was found that a sudden excursion from the stable equilibrium can cause the fast variable (the prey population density) to temporary collapse to exceedingly low values. Note that R-tipping is not the only mechanism in which transient dynamics can cause regime shifts. It has been shown that transients causing regime shifts are ubiquitous in ecological systems (51–55) with significant management implications (56, 57).

D. Noise in ecological systems. Ecological systems are continually exposed to stochastic disturbances and the effects of noise on the dynamics of these systems have been a topic of study with a long history (28, 58–74). In general, there are two types of noises in ecological systems: external and internal, where the former can be modeled as additive Gaussian white noise (75, 76) and the latter are demographic or multiplicative noise (59, 66, 71, 77–79). Demographic noises as a manifestation of internal stochasticity are of particular importance to ecological systems due to the intrinsic uncertainties in reproduction, growth, death, competition, and intraspecific migration. Computationally, a demographic process can be modeled as multiplicative noise with its strength proportional to the square root of the fluctuating abundance. In the context of tipping, the beneficial role of noise in facilitating species recovery after a tipping event was recognized (28, 29).

2. Carbon-cycle system: positive feedback loop in climate dynamics

In climate dynamics, a positive feedback loop called the climate-carbon cycle can arise: the release of CO_2 or other greenhouse gases into the atmosphere can increase the global temperature, but the latter can strengthen the climate driving forces that can amplify the CO_2 released into the atmosphere through peat decomposition. The essential nonlinear dynamics governing the feedback phenomenon, also known as the compost-bomb instability, can be modeled by a prototype of a carbon-temperature

system proposed in 2011 (80) with the key prediction that the instability depends strongly on the rate of global warming. Subsequently, this model was found to belong to the general class of the so-called type-B excitable systems (16), where an analytical solution indicated that, if the excitable system has a ramped parameter with an asymptotically stable equilibrium and a locally folded critical (slow) manifold, a critical value of the ramping rate can arise, above which an excitable response occurs.

Differing from the ecosystems, here we employ additive noise to illustrate that the phenomenon of rare events is general in fast-slow and excitable systems, regardless of the nature of the noise (i.e., multiplicative or additive). Specifically, we demonstrate that a nonautonomous climate-carbon cycle system subject to environmental noise with a time-varying parameter can exhibit the phenomenon of rare rarity. We consider the carbon-temperature model with the parameter values from Ref. (80), where global warming is modeled by an atmospheric temperature ramp, as shown in Fig. S1(A). The nonautonomous dynamical system is described by

$$\epsilon \dot{T} = C r_0 e^{\alpha T} - \frac{\lambda}{A}(T - T_a) + \xi_T^2 \quad [1a]$$

$$\dot{C} = B - C r_0 e^{\alpha T} + \xi_C^2 \quad [1b]$$

$$\dot{T}_a = \begin{cases} r & if \quad T_{a_{\min}} < T_a < T_{a_{\max}} \\ 0 & \text{otherwise,} \end{cases} \quad [1c]$$

where C and T are the vertically integrated soil carbon content and soil temperature, respectively, parameter B is the rate of increasing carbon by litter fall from plants and its value can decrease by microbial decomposition proportional to the exponential temperature (we fix $B = 1.055$), $r_0 = 0.02$ is the specific soil respiration rate, $\lambda = 5.049$ is the soil-to-atmosphere heat transfer coefficient, the three scaling parameters are $\alpha = \ln(3.5)/10$, $\epsilon = 0.175$, $A = 39$, and $\xi_{T,C}$ is the noise amplitude. Due to the considerable variation in the time scales of variables, the system described by Eq. Eq. (1) can be classified as an extremely stiff system. The pronounced imbalance in the ratio of fast to slow time scales can lead to inherent instability in numerical solutions. This imbalance poses a challenge for standard numerical methods in accurately capturing the dynamics of extremely stiff systems. Consequently, it is necessary to consider specialized techniques or implicit methods to enhance accuracy. In our work, we employ an implicit stochastic Runge–Kutta method (81–83) to integrate the system Eq. (1). (The algorithmic details are presented in Appendix 3.)

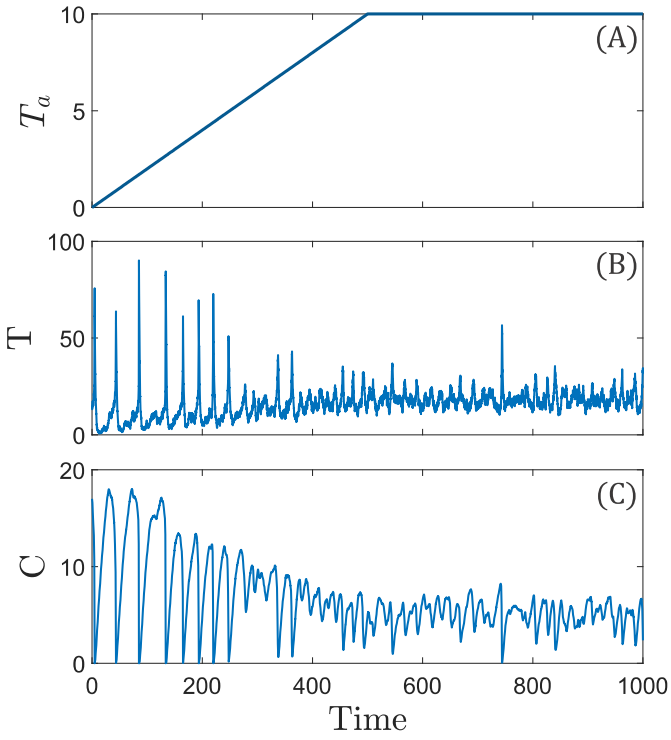

Fig. S1. Time trajectory of the nonautonomous system Eq. (1). (A) T_a (B) T (C) C for initial condition $(T_0, C_0, T_{a_0}) = (14, 17, 0)$ for $r = 0.02$, $T_{a_{\min}} = 0$, and $T_{a_{\max}} = 10$.

To be concrete, we assume that the range of temperature variation is $T_{a_{\min}} = 0$ and $T_{a_{\max}} = 10$, as shown in Fig. S1(A). The corresponding time series of $T(t)$ and $C(t)$ are shown in Figs. S1(B) and S1(C), respectively. It can be seen that the carbon concentration $C(t)$ exhibits the phenomenon of rare rarity. Similar to the slow-fast predator-prey system, noise induces

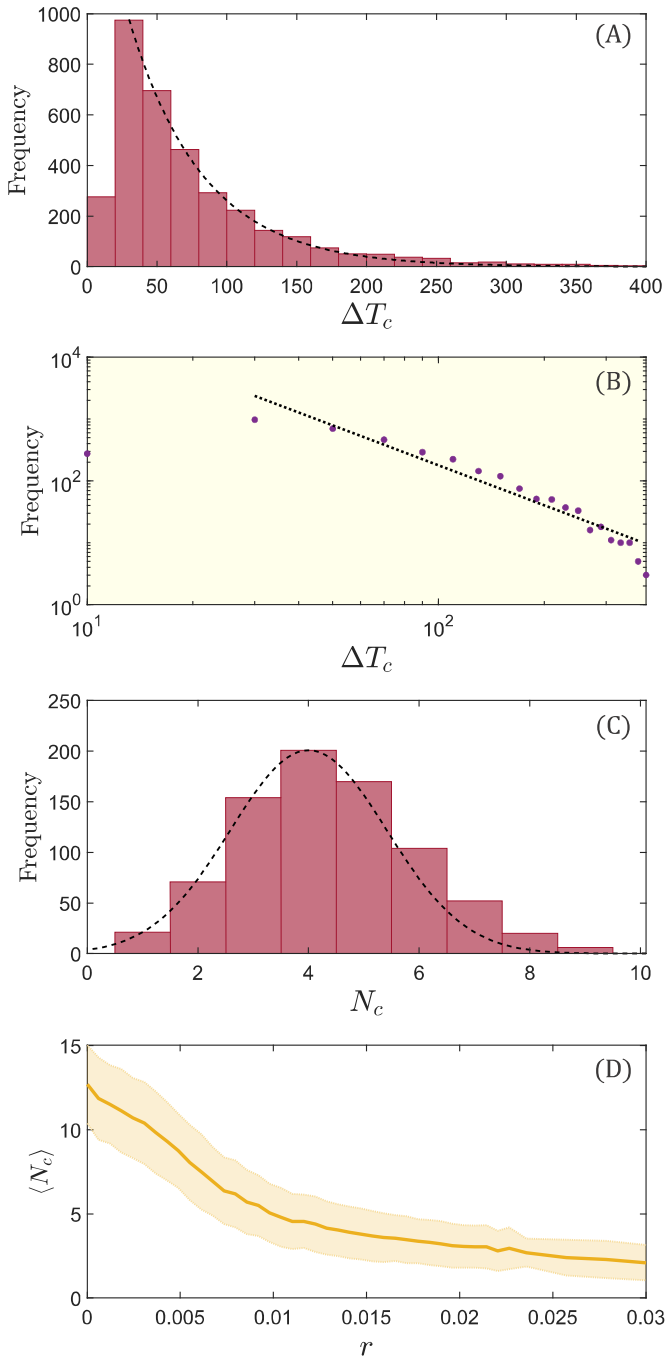

Fig. S2. Statistical behaviors of rare rarity events in the climate-carbon cycle system. (A) Distribution of the time interval ΔT_c between two chronologically adjacent rare rarity events and (B) distribution of the number N_c of rare rarity events, for $r = 0.012$, $T_{a_{\min}} = 0$, and $T_{a_{\max}} = 10$. (c) Mean value $\langle N_c \rangle$ of rare rarity events versus r, where the shaded area represents the standard deviation from the average. The larger value of rate r, the smaller number of rare rarity events in the climate-carbon cycle system Eq. (1).

intermittent occurrences of rare rarity. For low atmosphere temperatures, multiple rare rarity events can occur in short intervals, leading to potentially catastrophic outcomes. However, as the atmospheric temperature increases, there is a decline in the occurrence of such events, resulting in longer intervals between successive events. The distribution of the time interval between two consecutive events is approximately power-law and the number of such events can be modeled as a Gaussian random variable, as shown in Figs. S2(A) and S2(B), respectively. Figure S2(C) shows the mean value $\langle N_c \rangle$ associated with rare rarity events versus the rate r of linear temperature increase. As the atmospheric temperature T_a increases, the compost decomposition becomes more robust to noise, with the probability of experiencing multiple rare rarity events decreasing to near zero. This indicates that global warming can have a significant impact on the dynamics of the climate-carbon cycle system,

with higher atmospheric temperatures leading to more robust and stable compost decomposition in the cycle.

In the context of carbon-cycle dynamics, a rarity event represents an unexpected and potentially catastrophic excursive transient behavior that can lead to a drastic reduction in the soil carbon content and a corresponding increase in the emission of carbon into the atmosphere. However, when there is a global warming trend in which the atmospheric temperature T_a increases linearly from $T_{a_{\min}}$ to $T_{a_{\max}}$ at a constant rate r, the number of excursive transient collapses in soil carbon content decrease, accompanied by an increase in the interval between two consecutive rarity events, as exemplified in Figs. S1(B) and S1(C). These findings suggest that, as the atmospheric temperature continues to increase, a reduction in soil carbon content can occur, but the probability of transient collapse reduces as well. The implication is that global warming can counter intuitively enhance the robustness of the climate-carbon cycle against environmental noise. More specifically, as the soil carbon content declines while the noise amplitude remains constant, fewer excursive rare rarity events (compost-bomb instability) are likely to occur. Overall, these results provide insights into the dynamics of the climate-carbon cycle system under different atmospheric temperature conditions, which are relevant to making effective mitigation and adaptation strategies for combating global warming.

3. Stochastic Runge-Kutta Method

Table S1. Butcher tableau of improved implicit SRK methods Eq. (3) **- list of coefficients**

c_1	$a_{11}\ \ a_{12}\ \cdots\ a_{1s}$	$b_{11}\ \ b_{12}\ \cdots\ b_{1s}$	
c_2	$a_{21}\ \ a_{22}\ \cdots\ a_{2s}$	$b_{21}\ \ b_{22}\ \cdots\ b_{2s}$	
$\vdots$	$\vdots\ \ \vdots\ \ \ddots\ \ \vdots$	$\vdots\ \ \vdots\ \ \ddots\ \ \vdots$	
c_s	$a_{s1}\ \ a_{s2}\ \cdots\ a_{ss}$	$b_{s1}\ \ b_{s2}\ \cdots\ b_{ss}$	
$\hat{c}_1$	$\hat{a}_{11}\ \ \hat{a}_{12}\ \cdots\ \hat{a}_{1s}$		
$\hat{c}_2$	$\hat{a}_{21}\ \ \hat{a}_{22}\ \cdots\ \hat{a}_{2s}$		
$\vdots$	$\vdots\ \ \vdots\ \ \ddots\ \ \vdots$		
$\hat{c}_s$	$\hat{a}_{s1}\ \ \hat{a}_{s2}\ \cdots\ \hat{a}_{ss}$		
	$\beta_1\ \ \beta_2\ \cdots\ \beta_s$	$\gamma_1\ \ \gamma_2\ \cdots\ \gamma_s$	$\eta_1\ \ \eta_2\ \cdots\ \eta_s$

Table S2. Coefficients of improved implicit SRK methods Eq. (3) **for** $s = 2$

$\frac{1}{3}$	$\frac{5}{12}\ \ -\frac{1}{12}$	$0\ \ 0$	
1	$\frac{3}{4}\ \ \frac{1}{4}$	$4\ \ 0$	
0	$0\ \ 0$		
1	$1\ \ 0$		
	$\frac{3}{4}\ \ \frac{1}{4}$	$0\ \ 1$	$1\ \ -1$

A nonautonomous dynamical system subject to multiplicative noise can generally be written as

$$\dot{x} = f(x) + \xi(t)g(x), \qquad [2]$$

where the deterministic dynamics of the system are described by a d-dimensional nonlinear function $f : R^d \to R^d$, the second term describes the demographic noise with $\xi(t)$ being a Gaussian random process, and the function $g(x)$ is also a d-dimensional function $g : R^d \to R^d$. For the climate-carbon cycle model Eq. (1), we have $g(x) = 1$.

For nonstiff deterministic differential equations, a commonly used method for solving the corresponding stochastic differential equations (SDE) is some second-order algorithm (81). However, if the deterministic equations are stiff, a more robust computational method such as the implicit stochastic Runge-Kutta (SRK) algorithm (82) can be used. Under the Itô–Taylor series expansion, the implicit integration method can be characterized by its extended Butcher tableau. For the case of multidimensional Itô SDEs, the enhanced implicit SRK method is described as

$$\begin{aligned} x_{n+1} = x_n &+ \sum_{i=1}^{s} \beta_i f(t_n + c_i\delta t, H_i)\delta t \\ &+ \sum_{i=1}^{s} \gamma_i g(t_n + \hat{c}_i\delta t, \hat{H}_i) I_r^{\delta t} \\ &+ \sum_{i=1}^{s} \eta_i g(t_n + \hat{c}_i\delta t, \hat{H}_i) \frac{I_{r_0}^{\delta t}}{\delta t}, \end{aligned} \qquad [3]$$

for $n = 0, 1, \cdots, N-1$ with stages:

$$H_i = x_n + \sum_{j=1}^{s} a_{ij} f(t_n + c_j \delta t, H_j)\delta t + \sum_{j=1}^{s} b_{ij} g(t_n + \hat{c}_j \delta t, \hat{H}_j) \frac{I_{r_0}^{\delta t}}{\delta t} \quad [4a]$$

$$\hat{H}_i = x_n + \sum_{j=1}^{s} \hat{a}_{ij} f(t_n + c_j \delta t, H_j)\delta t, \quad [4b]$$

where the increments $I_{r_0,r}$ are the mixed stochastic-classical integrals in the corresponding sub intervals $[t, t+h]$, which can be calculated in the following way. Starting from independent standard normally distributed random variables $\xi_r, \zeta_r \sim N(0, \delta t)$, one computes:

$$I_r = \delta t^{1/2} \xi_r \quad [5]$$

$$I_{r0} = \delta t^{3/2} (\zeta_r/\sqrt{3} + \xi_r)/2. \quad [6]$$

The Butcher tableau represents the coefficients of the improved SRK method, where the weights c_i and $\hat{c}_i$ are chosen such that $c = Ae$ and $\hat{c} = \hat{A}e$. The improved SRK method Eq. (3) is implicit (explicit) when the matrices A, B, and $\hat{A}$ are full (lower triangular) matrices.

References

1. SE Williams, Yvette M Williams, Jeremy VanDerWal, Joanne L Isaac, Luke P Shoo, and Christopher N Johnson. Ecological specialization and population size in a biodiversity hotspot: how rare species avoid extinction. *Proc. Nat. Acad. Sci. (USA)*, 106(supplement_2):19737–19741, 2009.
2. Geerat J Vermeij and Richard K Grosberg. Rarity and persistence. *Ecol. Lett.*, 21(1):3–8, 2018.
3. Cristian Román-Palacios and John J Wiens. Recent responses to climate change reveal the drivers of species extinction and survival. *Proc. Nat. Acad. Sci. (USA)*, 117(8):4211–4217, 2020.
4. Russell Lande. Risks of population extinction from demographic and environmental stochasticity and random catastrophes. *The American Naturalist*, 142(6):911–927, 1993.
5. John L Sabo and Leah R Gerber. Predicting extinction risk in spite of predator–prey oscillations. *Ecological Applications*, 17(5):1543–1554, 2007.
6. Ramesh Arumugam, Frédéric Guichard, and Frithjof Lutscher. Persistence and extinction dynamics driven by the rate of environmental change in a predator–prey metacommunity. *Theoretical Ecology*, 13(4):629–643, 2020.
7. Marten Scheffer. *Ecology of Shallow Lakes*. Springer Science & Business Media, 2004.
8. Marten Scheffer, Jordi Bascompte, William A Brock, Victor Brovkin, Stephen R Carpenter, Vasilis Dakos, Hermann Held, Egbert H Van Nes, Max Rietkerk, and George Sugihara. Early-warning signals for critical transitions. *Nature*, 461(7260): 53–59, 2009.
9. M. Scheffer. Complex systems: foreseeing tipping points. *Nature*, 467:411–412, 2010.
10. D. B. Wysham and A. Hastings. Regime shifts in ecological systems can occur with no warning. *Ecol. Lett.*, 13:464–472, 2010.
11. John M Drake and Blaine D Griffen. Early warning signals of extinction in deteriorating environments. *Nature*, 467(7314): 456–459, 2010.
12. J Michael T Thompson and Jan Sieber. Predicting climate tipping as a noisy bifurcation: a review. *Int. J. Bif. Chaos*, 21 (02):399–423, 2011.
13. Luonan Chen, Rui Liu, Zhi-Ping Liu, Meiyi Li, and Kazuyuki Aihara. Detecting early-warning signals for sudden deterioration of complex diseases by dynamical network biomarkers. *Sci. Rep.*, 2:342, 2012.
14. C. Boettiger and Alan Hastings. Quantifying limits to detection of early warning for critical transitions. *J. R. Soc. Interface*, 9:2527–2539, 2012.
15. Lei Dai, Daan Vorselen, Kirill S Korolev, and Jeff Gore. Generic indicators for loss of resilience before a tipping point leading to population collapse. *Science*, 336(6085):1175–1177, 2012.
16. P. Ashwin, S. Wieczorek, R. Vitolo, and P. Cox. Tipping points in open systems: bifurcation, noise-induced and rate-dependent examples in the climate system. *Phil. Trans. Roy. Soc. A*, 370:1166–1184, 2012.
17. T. M. Lenton, V. N. Livina, V. Dakos, E. H. van Nes, and M. Scheffer. Early warning of climate tipping points from critical slowing down: comparing methods to improve robustness. *Phil. Trans. Roy. Soc. A*, 370:1185–1204, 2012.
18. A. D. Barnosky, E. A. Hadly, J. Bascompte, E. L. Berlowand J. H. Brown, M. Fortelius, W. M. Getz, J. Harte, A. Hastings, P. A. Marquet, N. D. Martinez, A. Mooers, P. Roopnarine, G. Vermeij, J. W. Williams, R. Gillespie, J. Kitzes, C. Marshall, N. Matzke, D. P. Mindell, E. Revilla, and A. B. Smith. Approaching a state shift in earth's biosphere. *Nature*, 486:52–58, 2012.

19. C. Boettiger and A. Hastings. Tipping points: From patterns to predictions. *Nature*, 493:157–158, 2013.
20. Jason M Tylianakis and Camille Coux. Tipping points in ecological networks. *Trends. Plant. Sci.*, 19(5):281–283, 2014.
21. J Jelle Lever, Egbert H Nes, Marten Scheffer, and Jordi Bascompte. The sudden collapse of pollinator communities. *Ecol. Lett.*, 17(3):350–359, 2014.
22. T. S. Lontzek, Y.-Y. Cai, K. L. Judd, and T. M. Lenton. Stochastic integrated assessment of climate tipping points indicates the need for strict climate policy. *Nat. Clim. Change*, 5:441–444, 2015.
23. S. Gualdia, M. Tarziaa, F. Zamponic, and J.-P. Bouchaudd. Tipping points in macroeconomic agent-based models. *J. Econ. Dyn. Contr.*, 50:29–61, 2015.
24. Junjie Jiang, Zi-Gang Huang, Thomas P Seager, Wei Lin, Celso Grebogi, Alan Hastings, and Ying-Cheng Lai. Predicting tipping points in mutualistic networks through dimension reduction. *Proc. Nat. Acad. Sci. (UsA)*, 115(4):E639–E647, 2018.
25. Biwei Yang, Meiyi Li, Wenqing Tang, Si Liu, Weixinand Zhang, Luonan Chen, and Jinglin Xia. Dynamic network biomarker indicates pulmonary metastasis at the tipping point of hepatocellular carcinoma. *Nat. Commun.*, 9:678, 2018.
26. Junjie Jiang, Alan Hastings, and Ying-Cheng Lai. Harnessing tipping points in complex ecological networks. *J. R. Soc. Interface*, 16(158):20190345, 2019.
27. Marten Scheffer. *Critical Transitions in Nature and Society*, volume 16. Princeton University Press, 2020.
28. Yu Meng, Junjie Jiang, Celso Grebogi, and Ying-Cheng Lai. Noise-enabled species recovery in the aftermath of a tipping point. *Phys. Rev. E*, 101:012206, Jan 2020. .
29. Yu Meng, Ying-Cheng Lai, and Celso Grebogi. Tipping point and noise-induced transients in ecological networks. *J. R. Soc. Interface*, 17(171):20200645, 2020.
30. Yu Meng and Celso Grebogi. Control of tipping points in stochastic mutualistic complex networks. *Chaos*, 31(2):023118, 2021.
31. Yu Meng, Ying-Cheng Lai, and Celso Grebogi. The fundamental benefits of multiplexity in ecological networks. *J. R. Soc. Interface*, 19:20220438, 2022.
32. Paul E O'Keeffe and Sebastian Wieczorek. Tipping phenomena and points of no return in ecosystems: beyond classical bifurcations. *SIAM J. Appl. Dyn. Syst.*, 19(4):2371–2402, 2020.
33. Richard Gomulkiewicz and Robert D. Holt. When does evolution by natural selection prevent extinction? *Evolution*, 49 (1):201–207, 1995. ISSN 00143820, 15585646. URL http://www.jstor.org/stable/2410305.
34. Christophe Trefois, Paul MA Antony, Jorge Goncalves, Alexander Skupin, and Rudi Balling. Critical transitions in chronic disease: transferring concepts from ecology to systems medicine. *Cur. Opin. Biotechnol.*, 34:48–55, 2015.
35. Katharina Albrich, Werner Rammer, and Rupert Seidl. Climate change causes critical transitions and irreversible alterations of mountain forests. *Global Change Biol.*, 26(7):4013–4027, 2020.
36. Atiyeh Bayani, Fatemeh Hadaeghi, Sajad Jafari, and Greg Murray. Critical slowing down as an early warning of transitions in episodes of bipolar disorder: A simulation study based on a computational model of circadian activity rhythms. *Chronobiol. Int.*, 34(2):235–245, 2017.
37. Peter Ashwin, Clare Perryman, and Sebastian Wieczorek. Parameter shifts for nonautonomous systems in low dimension: bifurcation-and rate-induced tipping. *Nonlinearity*, 30(6):2185, 2017.
38. Anna Vanselow, Sebastian Wieczorek, and Ulrike Feudel. When very slow is too fast-collapse of a predator-prey system. *J. Theo. Biol.*, 479:64–72, 2019.
39. U. Feudel. Rate-induced tipping in ecosystems and climate: the role of unstable states, basin boundaries and transient dynamics. *Nonlinear Proc. Geophys.*, 30(4):481–502, 2023. . URL https://npg.copernicus.org/articles/30/481/2023/.
40. Anna Vanselow, Lukas Halekotte, Pinaki Pal, Sebastian Wieczorek, and Ulrike Feudel. Rate-induced tipping can trigger plankton blooms. *Theo. Ecol.*, 2024. .
41. Alexis D Synodinos, Rajat Karnatak, Carlos A Aguilar-Trigueros, Pierre Gras, Tina Heger, Danny Ionescu, Stefanie Maaß, Camille L Musseau, Gabriela Onandia, Aimara Planillo, et al. The rate of environmental change as an important driver across scales in ecology. *Oikos*, page e09616, 2022.
42. Shirin Panahi, Younghae Do, Alan Hastings, and Ying-Cheng Lai. Rate-induced tipping in complex high-dimensional ecological networks. *Proc. Nat. Acad. Sci. (USA)*, 120(51):e2308820120, 2023.
43. Sebastian Wieczorek, Peter Ashwin, Catherine M Luke, and Peter M Cox. Excitability in ramped systems: the compost-bomb instability. *Proc. R. Soc. A Math. Phys. Eng. Sci.*, 467(2129):1243–1269, 2011.
44. James T Morris, PV Sundareshwar, Christopher T Nietch, Björn Kjerfve, and Donald R Cahoon. Responses of coastal wetlands to rising sea level. *Ecology*, 83(10):2869–2877, 2002.
45. Paul DL Ritchie, Hassan Alkhayuon, Peter M Cox, and Sebastian Wieczorek. Rate-induced tipping in natural and human systems. *Earth Syst. Dynam*, 14(3):669–683, 2023.
46. John Mitry, Michelle McCarthy, Nancy Kopell, and Martin Wechselberger. Excitable neurons, firing threshold manifolds and canards. *J. Math. Neurosci.*, 3(1):1–32, 2013.
47. NA Alexander, O Oddbjornsson, CA Taylor, HM Osinga, and David E Kelly. Exploring the dynamics of a class of post-tensioned, moment resisting frames. *J. Sound Vib.*, 330(15):3710–3728, 2011.
48. Sheng-Yi Hsu and Mau-Hsiang Shih. The tendency toward a moving equilibrium. *SIAM J. Appl. Dyn. Sys.*, 14(4): 1699–1730, 2015.
49. Andrew Morozov and Sergei Petrovskii. Excitable population dynamics, biological control failure, and spatiotemporal pattern formation in a model ecosystem. *Bull. Math. Biol.*, 71:863–887, 2009.

50. Tessa N Hempson, Nicholas AJ Graham, M Aaron MacNeil, Andrew S Hoey, and Shaun K Wilson. Ecosystem regime shifts disrupt trophic structure. *Ecol. Appl.*, 28(1):191–200, 2018.
51. A. Hastings and K. Higgins. Persistence of transients in spatially structured ecological models. *Science*, 263:1133–1136, 1994.
52. A. Hastings. Transient dynamics and persistence of ecological systems. *Ecol. Lett.*, 4:215–220, 2001.
53. A. Hastings. Transients: the key to long-term ecological understanding? *Trends Ecol. Evol.*, 19:39–45, 2004.
54. Alan Hastings, Karen C Abbott, Kim Cuddington, Tessa Francis, Gabriel Gellner, Ying-Cheng Lai, Andrew Morozov, Sergei Petrovskii, Katherine Scranton, and Mary Lou Zeeman. Transient phenomena in ecology. *Science*, 361(6406): eaat6412, 2018.
55. Andrew Morozov, Karen Abbott, Kim Cuddington, Tessa Francis, Gabriel Gellner, Alan Hastings, Ying-Cheng Lai, Sergei Petrovskii, Katherine Scranton, and Mary Lou Zeeman. Long transients in ecology: theory and applications. *Phys. life Rev.*, 32:1–40, 2020.
56. A. Hastings. Timescales and the management of ecological systems. *Proc. Nat. Acad. Sci. (USA)*, 113:14568–14573, 2016.
57. Tessa Francis, Karen Abbott, Kim Cuddington, Gabriel Gellner, Alan Hastings, Ying-Cheng Lai, Andrew Morozov, Sergei Petrovskii, and Mary Lou Zeeman. Management implications of long transients in ecological systems. *Nat. Ecol. Evol.*, 5: 285–294, 2021.
58. Jonathan Roughgarden. A simple model for population dynamics in stochastic environments. *Ame. Naturalist*, 109(970): 713–736, 1975.
59. Joseph H Connell. Diversity in tropical rain forests and coral reefs: high diversity of trees and corals is maintained only in a nonequilibrium state. *Science*, 199(4335):1302–1310, 1978.
60. Russell Lande. Risks of population extinction from demographic and environmental stochasticity and random catastrophes. *Ame. Naturalist*, 142(6):911–927, 1993.
61. Q. Yao and H. Tong. On prediction and chaos in stochastic systems. *Philos. Trans. R. Soc. Lond. A*, 348:357–369, 1994.
62. Donald Ludwig. The distribution of population survival times. *Ame. Naturalist*, 147:506–526, 1996.
63. Jörgen Ripa, Per Lundberg, and Veijo Kaitala. A general theory of environmental noise in ecological food webs. *Ame. Naturalist*, 151(3):256–263, 1998.
64. Russell Lande. Demographic stochasticity and allee effect on a scale with isotropic noise. *Oikos*, 83:353–358, 1998.
65. Brian Dennis. Allee effects in stochastic populations. *Oikos*, 96(3):389–401, 2002.
66. Michael B. Bonsall and Alan Hastings. Demographic and environmental stochasticity in predator–prey metapopulation dynamics. *J. Animal Ecol.*, 73(6):1043–1055, 2004.
67. S. P. Ellner and P. Turchin. When can noise induce chaos and why does it matter: A critique. *Oikos*, 111:620–631, 2005.
68. Ying-Cheng Lai and Yi-Rong Liu. Noise promotes species diversity in nature. *Phys. Rev. Lett.*, 94:038102, Jan 2005. .
69. Ying-Cheng Lai. Beneficial role of noise in promoting species diversity through stochastic resonance. *Phys. Rev. E*, 72(4): 042901, 2005.
70. V. Guttal and C. Jayaprakash. Impact of noise on bistable ecological systems. *Ecol. Model.*, 201:420–428, 2007.
71. Lasse Ruokolainen, Andreas Lindén, Veijo Kaitala, and Mike S Fowler. Ecological and evolutionary dynamics under coloured environmental variation. *Trends. Ecol. Evol.*, 24(10):555–563, 2009.
72. S. C. Doney and S. F. Sailley. When an ecological regime shift is really just stochastic noise. *Proc. Nat. Acad. Sci. (USA)*, 110:2438–2439, 2013.
73. Ottar N. Bjornstad. Nonlinearity and chaos in ecological dynamics revisited. *Proc. Nat. Acad. Sci. (USA)*, 112:6252–6253, 2015.
74. S. M. O'Regan. How noise and coupling influence leading indicators of population extinction in a spatially extended ecological system. *J. Biol. Dyn.*, 12:211–241, 2018.
75. Mikko Heino. Noise colour, synchrony and extinctions in spatially structured populations. *Oikos*, 83:368–375, 1998.
76. Timothy Guy Benton, CT Lapsley, and Andrew P Beckerman. The population response to environmental noise: population size, variance and correlation in an experimental system. *J. Animal Ecol.*, 71:320–332, 2002.
77. Bryan T. Grenfell, Ottar N. Bjornstad, and B. F. Finkenstädt. Dynamics of measles epidemics: Scaling noise, determinism, and predictability with the tsir model. *Ecol. Monographs*, 72(2):185–202, 2002.
78. Paula Villa Martín, Juan A Bonachela, Simon A Levin, and Miguel A Muñoz. Eluding catastrophic shifts. *Proc. Nat. Acad. Sci. (USA)*, 112:E1828–E1836, 2015.
79. G. W. A. Constable, T. Rogers, A. J. McKane, and C. E. Tarnita. Demographic noise can reverse the direction of deterministic selection. *Proc. Nat. Acad. Sci. (USA)*, 113:E4745–E4754, 2016.
80. CM Luke and PM Cox. Soil carbon and climate change: from the jenkinson effect to the compost-bomb instability. *Eur. J. Soil Sci.*, 62(1):5–12, 2011.
81. Christian Van den Broeck, JMR Parrondo, Raúl Toral, and Ryoichi Kawai. Nonequilibrium phase transitions induced by multiplicative noise. *Phys. Rev. E*, 55(4):4084, 1997.
82. Evelyn Buckwar, Andreas Rößler, and Renate Winkler. Stochastic runge–kutta methods for itô sodes with small noise. *SIAM J. Sci. Comput.*, 32(4):1789–1808, 2010.
83. Andreas Rößler. Runge–kutta methods for the strong approximation of solutions of stochastic differential equations. *SIAM J. Numer. Anal.*, 48(3):922–952, 2010.